BIODIVERSITAS
Volume 27, Number 1, January 2026
Pages: 11

ISSN: 1412-033X
E-ISSN: 2085-4722
https://doi.org/10.13057/biodiv/d270145

Virulence traits and gene profiles of *Vibrio alginolyticus* from farmed red drum in Vietnam

NGUYEN NAM QUANG[1], NGUYEN DUC QUYNH ANH[1], NGUYEN THI HUE LINH[1], CAROLA VENTURINI[2], FRANSISCA SAMSING[2], NGUYEN NGOC PHUOC[1,♥]

[1]Faculty of Fisheries, University of Agriculture and Forestry, Hue University. 102 Phung Hung St., Hue City, Vietnam. Tel.: +84 234 3539531,
♥email: nguyenngocphuoc@hueuni.edu.vn
[2]Sydney School of Veterinary Science, Faculty of Science, University of Sydney. McMaster Building (B14), NSW 2006, Australia

Manuscript received: 23 October 2025. Revision accepted: 29 January 2026.

Abstract. *Quang NN, Anh NDQ, Linh NTH, Venturini C, Samsing F, Phuoc NN. 2026. Virulence traits and gene profiles of* Vibrio alginolyticus *from farmed red drum in Vietnam. Biodiversitas 27 (1): d270145. https://doi.org/10.13057/biodiv/d270145*. *Vibrio alginolyticus* is an emerging bacterial pathogen associated with hemorrhagic disease and mortality in red drum (*Sciaenops ocellatus*) and other marine fish species. This study investigated virulence phenotypes and virulence-associated gene profiles of *V. alginolyticus* isolates infecting red drum, which is strain-dependent and reflects the combined expression of multiple phenotypic traits rather than the presence of individual virulence genes alone. Twenty *V. alginolyticus* isolates obtained from diseased red drum farmed in Hue City, central Vietnam, were evaluated for swimming motility, extracellular enzyme activity, and biofilm formation, and a composite virulence score was calculated using min-max normalized phenotypic data. Based on these scores, ten high-ranking isolates were selected for PCR screening of sixteen virulence-associated genes. Marked phenotypic variability was observed among isolates, with motility and extracellular enzyme activity contributing most strongly to virulence differentiation, whereas biofilm formation was generally weak to moderate. Fifteen genes were detected, including flagellar and motility-related genes (*flaA, flaC, flgE, flrA, flrB, flrC,* and *flaK*), hemolysin-related genes (*trh* and *tlh*), an adhesion gene (*tcpA*), secretion system components (*vopB, vopD,* and *vgrG*), and iron-acquisition genes (*pvuA* and *pvsA*), whereas *tdh* was not detected. Among the isolates, VA15 and VA17 exhibited the highest motility and extracellular enzyme activities, while most isolates formed weak but detectable biofilms. Pathogenicity testing confirmed that isolate VA15, identified as the most virulent based on in vitro profiling, caused dose-dependent mortality in red drum, with an LD_{50} of 4.0×10^4 CFU/fish (95% CI: 3.2×10^4-5.1×10^4 CFU/fish). Overall, this study provides baseline phenotypic and molecular data on *V. alginolyticus* infecting farmed red drum in central Vietnam and contributes to understanding virulence variability among isolates in marine cage aquaculture systems.

Keywords: Aquaculture diseases, hemorrhagic disease, pathogenicity genes, Southeast Asian aquaculture, *Vibrio alginolyticus*

INTRODUCTION

The red drum (*Sciaenops ocellatus* (Linnaeus, 1766)) is an estuarine fish species native to the Atlantic Ocean that has become an economically important mariculture species due to its broad environmental tolerance and rapid growth (Ackerly et al. 2023). Global production of red drum reached approximately 77,000 tons in 2019, with an estimated value of USD 196 million, of which more than 90% was produced in China through intensive cage culture systems (Xiao et al. 2023). In Vietnam, red drum has been identified as a strategic species for marine aquaculture development toward 2030, with a vision to 2045 (MARD 2021), and is currently farmed in several coastal provinces, including Hue City in central Vietnam (Linh et al. 2022). However, the rapid expansion of red drum farming has been accompanied by increasing reports of bacterial diseases, particularly those caused by *Vibrio* species.

Despite its commercial importance, red drum remains susceptible to several major bacterial pathogens, including *Streptococcus iniae* (Mmanda et al. 2014), *Nocardia seriolae* (Del Río-Rodríguez et al. 2021), and *Vibrio alginolyticus*. Among these, *V. alginolyticus* has been increasingly recognized as a primary etiological agent of hemorrhagic disease outbreaks in farmed red drum in Vietnam and its pathogenicity is highly strain dependent, with marked variability in virulence traits and disease severity observed among isolates, underscoring the need for detailed characterization of strains circulating in local farming systems (Linh et al. 2022). Such outbreaks are often associated with high stocking densities and fluctuating environmental conditions typical of marine cage culture systems, which may exacerbate host susceptibility and pathogen virulence.

Vibrio alginolyticus is a Gram-negative, motile bacterium widely distributed in estuarine and coastal environments worldwide (Baker-Austin et al. 2018). Its pathogenicity is multifactorial and involves a combination of phenotypic traits, including motility, extracellular enzyme production, and biofilm formation, which facilitate host colonization, tissue invasion, and environmental persistence. However, the variability of these virulence-associated phenotypes among *V. alginolyticus* isolates infecting red drum in Vietnam has not been systematically evaluated. Moreover, understanding the combined expression of these phenotypic traits is essential for explaining differences in disease severity observed under farm conditions. Differences in the

expression of these traits among strains may partly explain the inconsistent disease outcomes reported across farms and production cycles.

In addition to phenotypic traits, *V. alginolyticus* harbors numerous virulence-associated genes involved in adhesion, cytotoxicity, immune modulation, and nutrient uptake. These include genes related to hemolytic activity, motility and chemotaxis, secretion systems, and iron acquisition, which collectively contribute to host colonization and pathogenicity (Hernández-Robles et al. 2016; Echazarreta and Klose 2019; Yen et al. 2021; Tanabe et al. 2025). While these gene families have been reported in *V. alginolyticus* isolated from shrimp, bivalves, and environmental sources, their distribution among strains infecting fish, particularly red drum, remains poorly characterized.

Despite the frequent occurrence of hemorrhagic disease in red drum farms in central Vietnam, studies integrating phenotypic virulence profiling with molecular characterization of *V. alginolyticus* remain limited. Most previous investigations have focused on individual virulence traits or selected genes in isolation, without assessing their combined contribution to pathogenicity. Moreover, in vivo pathogenicity validation, particularly LD_{50} determination in the target host species, has rarely been reported for *V. alginolyticus* isolates from Vietnam. Consequently, the virulence potential and heterogeneity of strains circulating in local red drum farming systems remain insufficiently understood. This knowledge gap limits the development of effective disease management and prevention strategies for red drum aquaculture in Vietnam.

In this context, the present study aimed to characterize key virulence phenotypes, including motility, extracellular enzyme activity, and biofilm formation, and to detect virulence-associated genes in *V. alginolyticus* isolated from diseased red drum farmed in central Vietnam. The study further integrated phenotypic assays, PCR-based gene detection, and in vivo pathogenicity testing in the target host species. This study provides region-specific baseline data on virulence variability among *V. alginolyticus* isolates and contributes to a better understanding of pathogenic mechanisms relevant to marine cage aquaculture of red drum.

MATERIALS AND METHODS

Study area

Red drum (*Sciaenops ocellatus*) displaying clinical signs of hemorrhagic disease, including skin ulceration, scale loss, fin erosion, and subcutaneous hemorrhage, were collected from six marine cage-culture farms (three farms in Phu Loc commune and three farms in Phu Vang commune), Hue City, central Vietnam. Sampling was conducted during two periods, March and April 2024 (Figure 1). A total of 20 diseased fish were collected (8 fish in March and 12 fish in April), representing the typical size classes cultured at these farms (total length 25-40 cm; body weight 370-600 g).

Vibrio alginolyticus isolates

Twenty independent *V. Alginolyticus* isolates (VA01-VA20) were obtained, with one isolate recovered from each diseased fish to ensure isolate independence. Bacterial colonies were initially isolated on thiosulfate citrate bile salts sucrose agar (TCBS; Himedia, India) and subsequently purified on tryptone soy agar (TSA; Himedia, India) supplemented with 2% NaCl. Preliminary identification was performed using the API 20E system (bioMérieux, France). Species-level identification was confirmed by matrix-assisted laser desorption/ionization time-of-flight mass spectrometry (MALDI-TOF MS; Bruker Biotyper) at the University of Sydney, with a log(score) ≥2.0 considered reliable for species assignment.

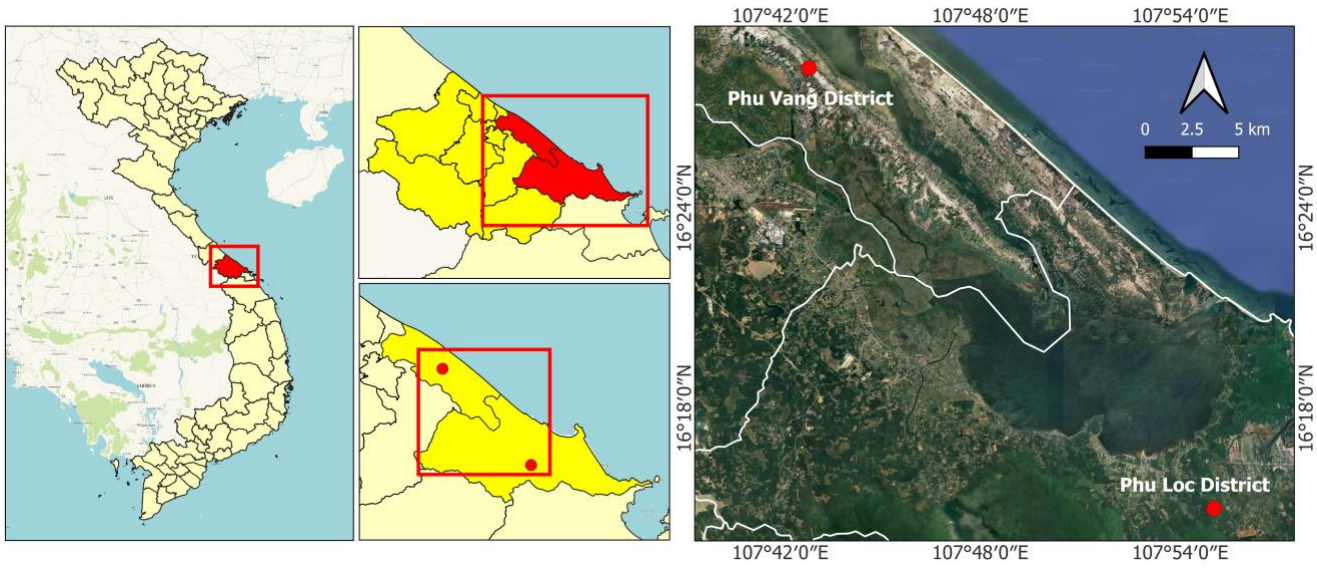

Figure 1. Location of the sampling sites in Phu Vang commune (16°28′12″N, 107°42′52″E) and Phu Loc commune (16°15′00″N, 107°55′01″E), Hue City, Vietnam

In vitro virulence phenotype assessment

Motility assay

Swimming motility was assessed following a modified protocol described by Partridge (2022). Briefly, soft-agar motility medium was prepared using Tryptone Soy Broth (TSB; Himedia, India) supplemented with 2% NaCl and 0.3% agar. A 1 µL aliquot of bacterial suspension standardized to OD_{600} = 0.5 was inoculated at the center of each agar plate and incubated at 28°C for 24 h. Swimming motility was quantified by measuring the diameter (mm) of the migration halo formed around the inoculation point.

Extracellular enzyme activity assay

Extracellular enzyme activities were assessed following Bunpa et al. (2016) with minor modifications. Isolates were grown on TSA supplemented with 2% NaCl at 28°C for 24 h. Enzyme-specific media were prepared by supplementing TSA with 1% (v/v) skim milk (caseinase), 1% (v/v) Tween 80 (lipase), 1% (v/v) egg yolk emulsion (phospholipase C), or 5% (v/v) sheep blood (hemolysin).

A 100 µL aliquot of log-phase bacterial suspension (OD_{600} = 0.5) was spot-inoculated at the center of each agar plate to produce a localized growth spot. Plates were incubated at 28°C for 48 h, after which reaction zones surrounding the growth spot were measured. Enzyme activity was quantified using an enzyme activity index defined as the ratio between the diameter of the Clearing or Opalescent Zone (CZ or OZ) and the diameter of the bacterial growth spot (CD). Caseinase activity was indicated by transparent clearing zones, lipase and phospholipase C activities by opalescent zones, and hemolytic activity by visible hemolysis on blood agar. Isolates without detectable reaction zones were classified as non-hemolytic (γ-hemolysis).

Biofilm formation assay

Biofilm formation was quantified using the crystal violet microtiter plate assay following Mitsuwan et al. (2025) with minor modifications. Isolates were cultured in TSB supplemented with 2% NaCl at 28°C with shaking (150 rpm) for 24 h, adjusted to OD_{600} = 1.0, and diluted to approximately 10^6 CFU mL^{-1}. Aliquots of 200 µL were transferred into sterile 96-well microtiter plates and incubated statically at 28°C for 24 h.

After incubation, wells were washed twice with phosphate-buffered saline (PBS, pH 7.4), air-dried, fixed with 95% ethanol, and stained with 0.1% (w/v) crystal violet. Bound dye was solubilized with 200 µL of 100% Dimethyl Sulfoxide (DMSO), selected due to its high and consistent solubilization efficiency for crystal violet under the assay conditions. Absorbance was measured at 570 nm. Negative-control wells containing sterile TSB were processed in parallel.

The cutoff Optical Density (ODc) was calculated as:

$$ODc = \text{mean}(OD_{570} \text{ of negative control}) + 3 \times SD$$

Biofilm production was classified according to Stepanović et al. (2000). All assays were performed with three biological replicates and three technical replicates.

Composite virulence score

Virulence potential was assessed based on three phenotypic traits: swimming motility, extracellular enzyme production, and biofilm formation. For each isolate, a mean enzyme activity index was first calculated across all tested enzymes. Each phenotypic trait was then normalized using min-max normalization according to the following formula:

$$N = \frac{X - Xmin}{Xmax - Xmin}$$

Where X represents the mean value of a given phenotypic trait for an isolate across replicates, and X_{min} and X_{max} are the minimum and maximum values of that trait observed among all isolates, respectively.

The composite virulence score was calculated as:

$$\text{Composite score} = N_{motility} + N_{enzyme} + N_{biofilm}$$

Yielding a theoretical range from 0 to 3. The ten isolates with the highest composite scores were selected for subsequent virulence gene screening.

Detection of virulence genes

Genomic DNA of *V. alginolyticus* was extracted from the ten isolates with the highest composite virulence scores using the QIAamp DNA Mini Kit (Qiagen, Germany) at the DNA Sequencing Company (Can Tho, Vietnam), following the manufacturer's instructions. DNA concentration and purity were assessed using a NanoDrop 2000 spectrophotometer (Thermo Scientific, USA).

PCR amplification was performed using a Bio-Rad T100™ thermal cycler with a 2× PCR master mix (Thermo Fisher Scientific, USA) and gene-specific primer pairs (Table 1). The PCR program consisted of an initial denaturation at 94°C for 5 min, followed by 35 cycles of denaturation at 94°C for 30 s, annealing at gene-specific temperatures (listed in Table 1) for 30 sec, and extension at 72°C for 45 sec, with a final extension at 72°C for 5 min.

PCR products were resolved by electrophoresis on 2% (w/v) agarose gels prepared in 1× TAE buffer and run at 100 V for 20 min. Gels were stained with GelRed and visualized using the runVIEW™ gel documentation system. A GeneRuler™ 100 bp Plus DNA Ladder (Thermo Scientific, USA) was used as a molecular size marker. Positive controls consisted of genomic DNA from the reference *V. alginolyticus* strain ATCC 17749, while negative controls contained nuclease-free water in place of template DNA.

Pathogenicity assay and LD_{50} determination

Based on phenotypic screening, isolate VA15, which exhibited the highest composite virulence score, was selected as a representative high-virulence strain for in vivo pathogenicity assessment.

Table 1. Primer sequences, annealing temperatures, and expected amplicon sizes used for PCR detection of virulence-associated genes in *Vibrio alginolyticus*

Targeted gene	Primer	Sequence (5'-3')	Ta (°C)	Product size (bp)	References
tlh	TLH-L	AAAGCGGATTATGCAGAAGCACTG	55	369	Park et al. (2024)
	TLH-R	GCTACTTTCTAGCATTTTCTCTGC			
trh	TRH-L	TTGGCTTCGATATTTTCAGTATCT	56	486	Park et al. (2024)
	TRH-R	CATAACAAACATATGCCCATTTCCG			
tdh	TDH-L	GTAAAGGTCTCTGACTTTTGGAC	57	270	Park et al. (2024)
	TDH-R	TGGAATAGAACCTTCATCTTCACC			
tcpA	tcpA-F	CACGATAAGAAAACCGGTCCAAGAG	58	451	Islam et al. (2005)
	tcpA-R	ACCAAATGCAACGCCGAATGGAGC			
flaA	A1-F	TCAGGTCAATACAAATATCAATGC	52	1062	Madhi et al. (2013)
	A1-R	CTGCTAACACGCCAATCC			
flaC	flaC-F	ATGGCTGTAACAGTTAGTACT	52	1099	Liang et al. (2010)
	flaC-R	TTACTGCAATAGTGACATTGC			
flgE	flgE-F	GGAATGAAGTTTTTAGGGAAGTACG	54	137	Li et al. (2022)
	flgE-R	CTGGTAAGTATACATGCTCTTCTCG			
flaK	flaK-F	CGATTTGTAGTCTGCTGCTG	52	897	Bardy et al. (2002)
	flaK-R	TTGCTGGTATAGGCTGATGT			
vopB	*vopB*-F	GAAAGGCGTAACGGACAA	55	225	Hernández-Robles et al. (2016)
	vopB-R	CAGGACGGCTTAACACCG			
vopD	*vopD*-F	GATAAAAATGGTGGAACGGG	55	400	Hernández-Robles et al. (2016)
	vopD-R	CGTTCTTCGGCTTGGTTT			
vgrG	*vgrG-F*	GAAGACGAAGCGAACCAAG	55	532	Hernández-Robles et al. (2016)
	vgrG-R	ATTGAACCATCACTGTTCATCAC			
pvsA	*pvsA-F*	AGCCGCCTTACTTTATCG	50	467	Hernández-Robles et al. (2016)
	pvsA-R	CGAGACAATCGAAATTCG			
pvuA	*pvuA-F*	AATTGCCTACATCCGAGG	52	545	Hernández-Robles et al. (2016)
	pvuA-R	CAACATTCATGCGTAACTTG			
flrA	*flrA-F*	ATGAGCGATGACAACAACAA	55	883	Luo et al. (2016)
	flrA-R	TTAGCTGGTGTTGTTCAGGT			
flrB	*flrB-F*	CCAAATCTTCCTCCAGCGACA	55	756	Luo et al. (2016)
	flrB-R	CTACCAACTGGGCAATCGTGAAT			
flrC	*flrC-F*	AGCGAAGTTGTTGCGTGTTTT	60	894	Luo et al. (2016)
	flrC-R	GCGGTAATATAAGTCCTCTCTGA			

Juvenile red drum (*S. ocellatus*; body weight 8-10 g) were acclimated for two weeks prior to the experiment and maintained in 120 L plastic tanks at a stocking density of 30 fish per tank, with three replicate tanks per treatment. Fish were reared in seawater with a salinity of 25-30 ppt at 27±1°C, pH 7.8-8.2, and dissolved oxygen levels above 6 mg L^{-1}. Five experimental groups were intraperitoneally injected with 0.1 mL of bacterial suspension at doses of 10^3-10^7 CFU $fish^{-1}$, while control fish received sterile PBS.

Fish were anesthetized using AQUI-S (20 mg L^{-1}) prior to injection. Humane endpoints were defined as loss of equilibrium, inability to maintain swimming posture, unresponsiveness to external stimuli, or severe respiratory distress. Fish meeting these criteria were humanely euthanized and recorded as mortalities. Mortality was monitored daily for 14 days post-challenge. *Vibrio alginolyticus* was re-isolated from dead or euthanized fish on HiCrome™ Vibrio Agar and confirmed by API 20E. The median Lethal Dose (LD_{50}) was calculated using the Reed-Muench method (Reed and Muench 1938).

All experimental procedures involving animals were conducted in strict accordance with institutional and national guidelines and were approved by the Animal Ethics Committee of Hue University (Approval No. HUVN0054, 2024).

Statistical analysis

Quantitative phenotype data, including swimming halo diameters, hemolytic clearing zones, lipase opalescent zones, and OD_{570} values obtained from the 20 *V. alginolyticus* isolates, were expressed as mean±Standard Deviation (SD). Prior to analysis, data were assessed for normality using the Shapiro-Wilk test and for homogeneity of variances using Levene's test. When required to meet ANOVA assumptions, data were log- or square-root-transformed; otherwise, untransformed data were used.

Differences among isolates were evaluated using one-way Analysis of Variance (ANOVA), followed by Tukey's Honestly Significant Difference (HSD) post hoc test for pairwise comparisons. Effect sizes (η^2) were reported where appropriate. A significance level of $p<0.05$ was applied for all tests. Survival data were analyzed using Kaplan-Meier survival curves, and differences among challenge doses were evaluated using the log-rank (Mantel-Cox) test. All statistical analyses were performed using IBM SPSS Statistics version 20.

RESULTS AND DISCUSSION

Virulence phenotypes assessment

Motility

All *V. alginolyticus* isolates examined (n = 20) exhibited detectable swimming motility on soft agar (Figure 2.A; Table 2). Swimming halo diameters differed significantly among isolates (One-Way ANOVA, $p<0.05$), indicating marked phenotypic variability. The highest motility was recorded in isolates VA15 and VA17 (24.33±0.58 mm; Tukey group "a"), followed by VA08, VA10, VA11, VA04, VA05, VA01, and VA18 (23.00-24.00 mm; Tukey groups "a-ab"; Table 2). In contrast, the lowest motility was observed in isolates VA09 and VA19 (17.33±0.58 mm; group "b"), with VA06, VA12, and VA13 also displaying significantly smaller migration halos than the highly motile isolates. These results demonstrate a wide but statistically structured variation in swimming ability among the isolates recovered from diseased red drum.

Extracellular enzymes

All isolates produced detectable levels of caseinase, lipase, phospholipase C, and β-hemolysin (Figures 2.B-2E; Table 2). Caseinase activity varied significantly among isolates ($p<0.05$), ranging from 1.68±0.05 (VA02, VA12) to 2.00±0.10 (VA18). Lipase activity showed a similar pattern, with VA15 and VA17 exhibiting the highest OZ/CD ratios (1.91-1.92), whereas VA12, VA13, and VA19 displayed the lowest values (approximately 1.73-1.74). Phospholipase C activity also differed significantly, ranging from 1.70±0.05 (VA02, VA06, VA12, VA14) to 1.89±0.01 (VA08, VA10, VA11, VA17). Overall, extracellular enzyme profiles revealed consistent clustering, with isolates VA15, VA17, VA10, VA11, and VA18 ranking among the highest performers across multiple enzyme categories, suggesting coordinated expression of extracellular degradative activities in these isolates.

Biofilm formation

Biofilm formation was detected in all isolates, with OD_{570} values ranging from 0.20 to 0.23 (Figure 2.F; Table 2). Negative-control wells produced low but non-zero OD_{570} values (0.004-0.010), allowing reliable calculation of the cutoff Optical Density (ODc) following Stepanović et al. (2000). Based on ODc classification, most isolates were categorized as weak biofilm producers, whereas a subset of isolates (including VA04, VA05, VA08, VA10, VA11, VA15, and VA17) approached or exceeded the moderate biofilm threshold. Although biofilm formation exhibited less variability than motility or enzyme activity, the consistent detection of biofilms across isolates indicates a conserved capacity for surface attachment under the in vitro conditions tested.

Hemolytic activity

β-hemolytic activity was observed in all isolates on sheep blood agar, with CZ/CD ratios ranging from 1.57±0.07 (VA03) to 1.92±0.09 (VA15) (Figure 2.C; Table 2). Isolates showing the strongest hemolytic activity included VA08, VA10, VA11, VA15, VA17, and VA18, which also ranked highly for other virulence-associated phenotypes. This concordance suggests that hemolytic capacity contributes to the overall virulence phenotype of these isolates.

Virulence score

Composite virulence scores, calculated from min-max normalized motility, mean enzyme activity, and biofilm formation values, ranged from 0.147 to 3.000 among the 20 isolates, reflecting substantial phenotypic heterogeneity (Table 3). Isolate VA15 exhibited the highest composite score (3.000), followed by VA17 (2.926), VA10 (2.911), VA08 (2.890), and VA05 (2.769). In contrast, the lowest scores were observed in isolates VA19 (0.147), VA13 (0.154), and VA09 (0.491).

Among the three traits, swimming motility contributed strongly to score differentiation, with high-ranking isolates showing normalized values of 0.81-1.00, whereas low-ranking isolates ranged from 0 to 0.14. Mean enzyme activity indices similarly distinguished isolates with strong proteolytic and lipolytic capacities from weaker performers. By comparison, biofilm formation showed relatively limited variation and therefore contributed more modestly to the overall ranking.

Based on these composite scores, the ten highest-ranking isolates (VA15, VA17, VA10, VA08, VA05, VA04, VA11, VA18, VA01, and VA07) were selected for subsequent PCR screening of virulence-associated genes (Table 3).

Virulence-associated genes screening

PCR screening of the ten *V. alginolyticus* isolates with the highest composite virulence scores revealed a largely conserved distribution of virulence-associated genes among the screened isolates (Table 4). Fifteen of the sixteen targeted genes were detected, whereas *tdh* was not amplified in any of the tested isolates. All screened isolates carried flagellar and motility-related genes (*flaA, flaC, flgE, flrA, flrB, flrC,* and *flaK*), indicating the presence of a complete flagellar biosynthesis and regulatory machinery. The ubiquitous detection of these genes is consistent with the strong swimming motility phenotypes observed among the high-ranking isolates in the phenotypic assays.

Genes associated with hemolytic activity (*trh* and *tlh*) were detected in all screened isolates, in agreement with the β-hemolytic phenotype observed on sheep blood agar. In contrast, *tdh*, a hemolysin gene more commonly associated with *Vibrio parahaemolyticus*, was absent. This finding is consistent with previous reports indicating that fish-associated *V. alginolyticus* strains typically rely on *trh* and *tlh* as major determinants of hemolytic activity.

All screened isolates also harbored the adhesion-related gene *tcpA*, along with secretion system-associated genes *vopB* and *vopD* (type III secretion system, T3SS) and *vgrG* (type VI secretion system, T6SS). In addition, the iron-acquisition genes *pvsA* and *pvuA*, which are involved in vibrioferrin biosynthesis and uptake, were consistently detected. The conserved presence of these genes suggests that the screened isolates share a common genetic repertoire supporting host colonization, effector delivery, and iron acquisition under iron-limited conditions typical of the host environment.

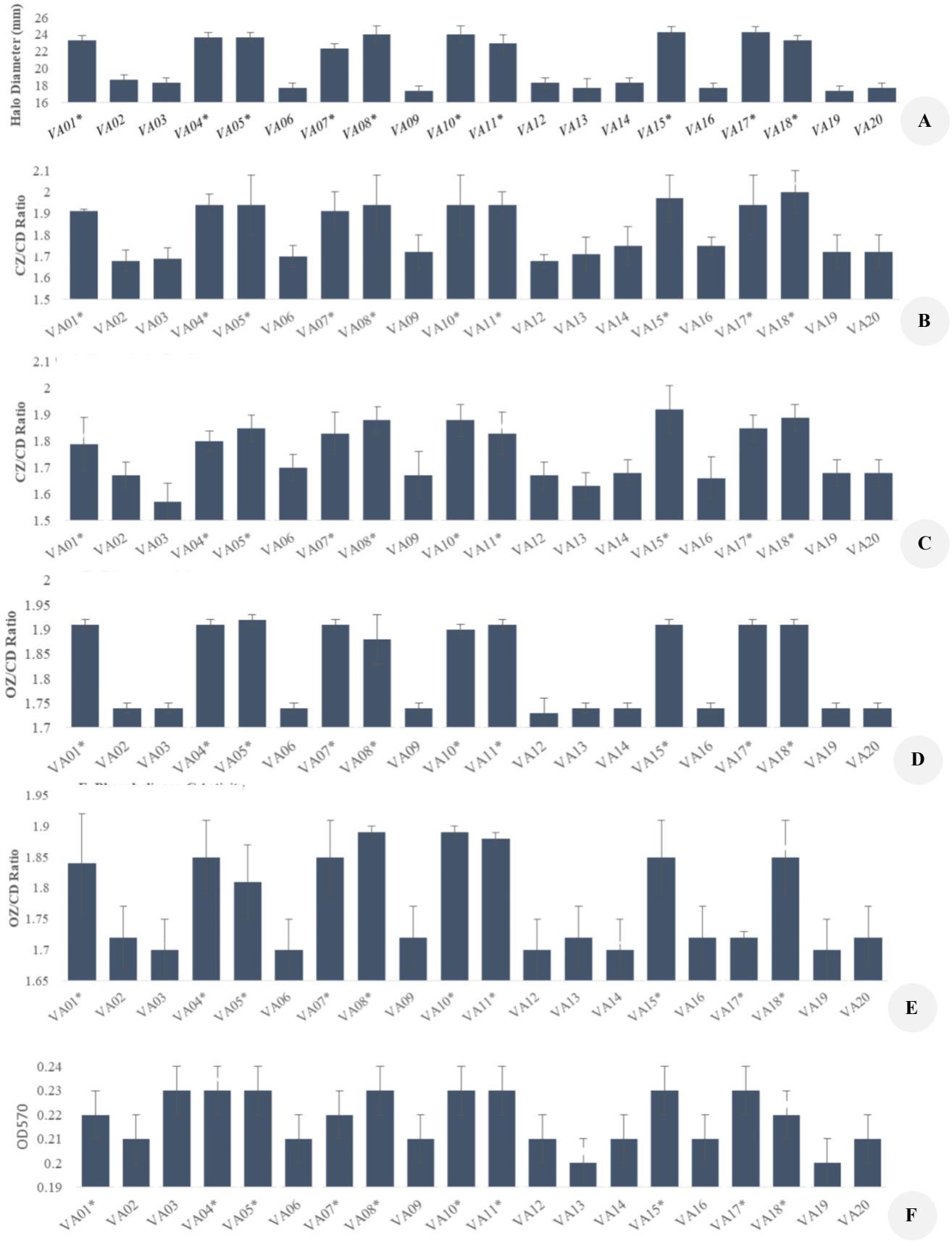

Figure 2. A. Swimming motility, B. Caseinase activity, C. β-hemolysin production, D. Lipase activity, E. Phospholipase-C activity, F. Biofilm formation of 20 *Vibrio alginolyticus* isolates

Table 2. Motility, extracellular enzyme activities, β-hemolysin production, and biofilm formation in *Vibrio alginolyticus* isolated from red drum with hemorrhagic disease

Isolates	Mean±SD					
	Swimming halo	Caseinase	β-Hemolysin	Lipase	Phospholipase-C	Biofilm
	Diameter (mm)	Rate CZ/CD		Rate OZ/CD		OD_{570}
VA01*	23.33^{a}±0.58	1.91^{abc}±0.01	1.79^{abcd}±0.10	1.91^{a}±0.01	1.84^{abc}±0.08	0.22^{abc}±0.01
VA02	18.67^{b}±0.58	1.68^{c}±0.05	1.67^{cde}±0.05	1.74^{b}±0.01	1.72^{bc}±0.05	0.21^{bc}±0.01
VA03	18.33^{b}±0.58	1.69^{c}±0.05	1.57^{e}±0.07	1.74^{b}±0.01	1.70^{c}±0.05	0.22^{abc}±0.01
VA04*	23.67^{a}±0.58	1.94^{abc}±0.05	1.80^{abcd}±0.04	1.91^{a}±0.01	1.85^{ab}±0.06	0.23^{a}±0.01
VA05*	23.67^{a}±0.58	1.94^{abc}±0.14	1.85^{abc}±0.05	1.92^{a}±0.01	1.81^{abc}±0.06	0.23^{a}±0.01
VA06	17.67^{b}±0.58	1.70^{bc}±0.05	1.70^{bcde}±0.05	1.74^{b}±0.01	1.70^{c}±0.05	0.21^{bc}±0.01
VA07*	22.33^{a}±0.58	1.91^{abc}±0.09	1.83^{abc}±0.08	1.91^{a}±0.01	1.85^{ab}±0.06	0.22^{ab}±0.01
VA08*	24.00^{a}±1.00	1.94^{abc}±0.14	1.88^{ab}±0.05	1.88^{a}±0.05	1.89^{a}±0.01	0.23^{a}±0.01
VA09	17.33^{b}±0.58	1.72^{bc}±0.08	1.67^{cde}±0.09	1.74^{b}±0.01	1.72^{bc}±0.05	0.21^{bc}±0.01
VA10*	24.00^{a}±1.00	1.94^{abc}±0.14	1.88^{ab}±0.06	1.90^{a}±0.01	1.89^{a}±0.01	0.23^{a}±0.01
VA11*	23.00^{a}±1.00	1.94^{abc}±0.06	1.83^{abc}±0.08	1.91^{a}±0.01	1.88^{a}±0.01	0.23^{a}±0.01
VA12	18.33^{b}±0.58	1.68^{c}±0.03	1.67^{cde}±0.05	1.73^{b}±0.03	1.70^{c}±0.05	0.21^{bc}±0.01
VA13	17.67^{b}±1.15	1.71^{bc}±0.08	1.63^{de}±0.05	1.74^{b}±0.01	1.72^{bc}±0.05	0.20^{ab}±0.01
VA14	18.33^{b}±0.58	1.75^{abc}±0.09	1.68^{cde}±0.05	1.74^{b}±0.01	1.70^{c}±0.05	0.21^{abc}±0.01
VA15*	24.33^{a}±0.58	1.97^{ab}±0.11	1.92^{a}±0.09	1.91^{a}±0.01	1.85^{ab}±0.06	0.23^{a}±0.01
VA16	17.67^{b}±0.58	1.75^{abc}±0.04	1.66^{cde}±0.08	1.74^{b}±0.01	1.72^{bc}±0.05	0.21^{bc}±0.01
VA17*	24.33^{a}±0.58	1.94^{abc}±0.14	1.85^{abc}±0.05	1.91^{a}±0.01	1.88^{a}±0.01	0.23^{a}±0.01
VA18*	23.33^{a}±0.58	2.00^{a}±0.10	1.89^{ab}±0.05	1.91^{a}±0.01	1.85^{ab}±0.06	0.22^{ab}±0.01
VA19	17.33^{b}±0.58	1.72^{bc}±0.08	1.68^{cde}±0.05	1.74^{b}±0.01	1.70^{c}±0.05	0.20^{ab}±0.01
VA20	17.67^{b}±0.58	1.72^{bc}±0.08	1.68^{cde}±0.05	1.74^{b}±0.01	1.72^{bc}±0.05	0.21^{bc}±0.01

Note: CD: Colony Diameter, OZ: Opalescent Zone diameter, CZ: Clearing Zone diameter, OD_{570}: Optical Density at 570 nm. Different superscript letters within the same column indicate significant differences among isolates (One-Way ANOVA followed by Tukey's HSD test, $p<0.05$). Values sharing at least one letter are not significantly different. Ten isolates (*) were selected for PCR analysis of virulence-associated genes

Table 3. Composite virulence scores of 20 *Vibrio alginolyticus* isolates based on motility, extracellular enzyme activities, and biofilm formation. Scores were calculated as the sum of min-max normalized values of each trait (range: 0-3), with higher values indicating greater virulence potential. Raw phenotypic measurements (motility in mm, enzyme indices, and biofilm OD) are presented for descriptive purposes, whereas only normalized components (0-1) were used to calculate composite scores at the individual-isolate level

Isolate	Motility (mm)	Caseinase	Lipase	Phospholipase	Hemolysin	Biofilm (OD_{570})	Mean enzyme index	Nmotility (0-1)	Nenzyme (0-1)	Nbiofilm (0-1)	Composite score	Rank
VA15	24.330	1.970	1.910	1.850	1.920	0.230	1.912	1.000	1.000	1.000	3.000	1
VA17	24.330	1.940	1.910	1.880	1.850	0.230	1.895	1.000	0.926	1.000	2.926	2
VA10	24.000	1.940	1.900	1.890	1.880	0.230	1.902	0.953	0.958	1.000	2.911	3
VA08	24.000	1.940	1.880	1.890	1.880	0.230	1.898	0.953	0.937	1.000	2.890	4
VA05	23.670	1.940	1.920	1.810	1.850	0.230	1.880	0.906	0.863	1.000	2.769	5
VA04	23.670	1.940	1.910	1.850	1.800	0.230	1.875	0.906	0.842	1.000	2.748	6
VA11	23.000	1.940	1.910	1.880	1.830	0.230	1.890	0.810	0.905	1.000	2.715	7
VA18	23.330	2.000	1.910	1.850	1.890	0.220	1.912	0.857	1.000	0.667	2.524	8
VA01	23.330	1.910	1.910	1.840	1.790	0.220	1.862	0.857	0.789	0.667	2.313	9
VA07	22.330	1.910	1.910	1.850	1.830	0.220	1.875	0.714	0.842	0.667	2.223	10
VA16	17.670	1.750	1.740	1.720	1.660	0.210	1.718	0.490	0.179	0.333	1.002	11
VA20	17.670	1.720	1.740	1.720	1.680	0.210	1.715	0.490	0.168	0.333	0.991	12
VA06	17.670	1.700	1.740	1.700	1.700	0.210	1.710	0.490	0.147	0.333	0.970	13
VA03	18.330	1.690	1.740	1.700	1.570	0.220	1.675	0.143	0.000	0.667	0.810	14
VA14	18.330	1.750	1.740	1.700	1.680	0.210	1.718	0.143	0.179	0.333	0.655	15
VA02	18.670	1.680	1.740	1.720	1.670	0.210	1.702	0.191	0.116	0.333	0.640	16
VA13	17.670	1.710	1.740	1.720	1.630	0.200	1.700	0.490	0.105	0.000	0.595	17
VA12	18.330	1.680	1.730	1.700	1.670	0.210	1.695	0.143	0.084	0.333	0.560	18
VA09	17.330	1.720	1.740	1.720	1.670	0.210	1.712	0.000	0.158	0.333	0.491	19
VA19	17.330	1.720	1.740	1.700	1.680	0.200	1.710	0.000	0.147	0.000	0.147	20

Table 4. PCR detection of virulence-associated genes in the ten *Vibrio alginolyticus* isolates with the highest composite virulence scores

Targeted gene	Phenotype	Isolate									
		VA15	VA17	VA10	VA08	VA05	VA04	VA11	VA18	VA01	VA07
flaA	Motility	+	+	+	+	+	+	+	+	+	+
flaC		+	+	+	+	+	+	+	+	+	+
flgE		+	+	+	+	+	+	+	+	+	+
flrA		+	+	+	+	+	+	+	+	+	+
flrB		+	+	+	+	+	+	+	+	+	+
flrC		+	+	+	+	+	+	+	+	+	+
flaK		+	+	+	+	+	+	+	+	+	+
tdh	Hemolysin	-	-	-	-	-	-	-	-	-	-
trh		+	+	+	+	+	+	+	+	+	+
tlh		+	+	+	+	+	+	+	+	+	+
tcpA	Pili	+	+	+	+	+	+	+	+	+	+
vopB	T3SS	+	+	+	+	+	+	+	+	+	+
vopD		+	+	+	+	+	+	+	+	+	+
vgrG	T6SS	+	+	+	+	+	+	+	+	+	+
pvuA	Iron acquisition	+	+	+	+	+	+	+	+	+	+
pvsA		+	+	+	+	+	+	+	+	+	+

Note: +: Indicates presence, and -: Indicates absence of PCR amplification for the corresponding target gene

Table 5. Cumulative mortality and onset of mortality (days post-infection) in red drum challenged with different doses of *Vibrio alginolyticus* isolate VA15

Dose (CFU fish^{-1})	Cumulative mortality (%)	Mortality onset period (dpi)
10^3	33.3±5.7	3-6
10^4	60.0±5.7	4-5
10^5	86.0±10.0	4-6
10^6	100	4-9
10^7	100	4-9

Note: Values are presented as mean±SD (n = 3 tanks per dose)

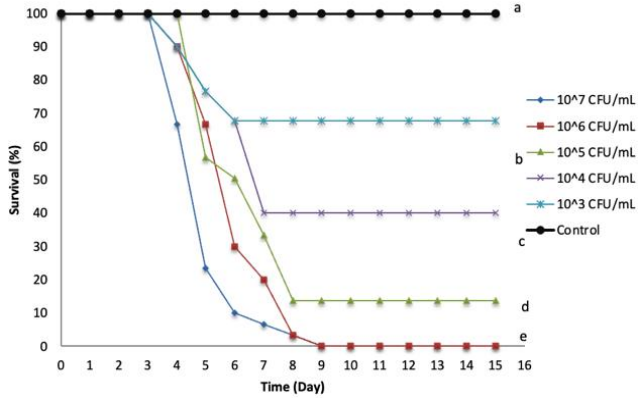

Figure 3. Survival of red drum challenged with different doses of *V. alginolyticus* isolate VA15. Fish were injected intraperitoneally with 10^3-10^7 CFU fish^{-1}, the control group received sterile PBS

Pathogenicity assay and LD_{50} determination

Isolate VA15, which exhibited the highest composite virulence score based on in vitro phenotypic profiling, was selected for in vivo pathogenicity assessment. Survival analysis revealed a clear dose-dependent increase in mortality among challenged groups compared with the control (log-rank test, $p<0.01$) (Figure 3).

Following intraperitoneal injection, cumulative mortality increased progressively with challenge dose. Mean cumulative mortality reached 33.3%, 60.0%, 86.0%, 100%, and 100% at doses of 10^3, 10^4, 10^5, 10^6, and 10^7 CFU fish^{-1}, respectively (Table 5). The onset of mortality occurred between 3 and 6 days post-infection (dpi) in fish challenged with 10^3 CFU fish^{-1}, 4-5 dpi at 10^4 CFU fish^{-1}, 4-6 dpi at 10^5 CFU fish^{-1}, and 4-9 dpi at the two highest challenge doses (10^6 and 10^7 CFU fish^{-1}). No additional mortality was observed beyond these time windows in any treatment group.

Using the Reed-Muench method, the median Lethal Dose (LD_{50}) of isolate VA15 was estimated at 4.0×10^4 CFU fish^{-1}, with a 95% confidence interval of 3.2×10^4-5.1×10^4 CFU fish^{-1}. This result confirms the high pathogenic potential of VA15 in juvenile red drum under the experimental conditions applied. Moribund fish exhibited gross pathological signs characteristic of vibriosis, including petechial and subcutaneous haemorrhages, fin erosion, pale liver, and moderate accumulation of abdominal fluid. *V. alginolyticus* was successfully re-isolated from 95-100% of sampled moribund fish, thereby fulfilling Koch's postulates and confirming the bacterial aetiology of observed mortalities.

Discussion

This study characterized virulence-related phenotypes and selected genetic features of *V. alginolyticus* isolated from diseased red drum in central Vietnam, providing insight into the multifactorial nature of pathogenicity in marine cage-culture systems. The examined isolates exhibited marked variability in swimming motility, extracellular enzyme production, biofilm formation, and hemolytic activity. Overall, these findings indicate that the virulence potential of fish-associated *V. alginolyticus* isolates examined in this study is not driven by a single dominant trait, but rather reflects the combined contribution of multiple

phenotypic characteristics that may act synergistically during infection.

Motility is a well-recognized virulence determinant in *Vibrio* species, facilitating host colonization, penetration of mucosal barriers, and early stages of infection (Phuoc et al. 2020; Sheikh et al. 2024). In the present study, isolates VA15 and VA17 displayed the highest swimming motility, which coincided with elevated expression of other virulence-associated phenotypes. Such coordinated expression of motility and additional virulence traits has been described in several *Vibrio* pathogens and is thought to reflect hierarchical regulation within the flagellar gene cascade. Moreover, strain-dependent variation in motility has been widely reported for *V. alginolyticus* isolated from both fish and shrimp culture systems (Ayuningrum et al. 2023), potentially arising from genetic diversity as well as environmental adaptation prior to host infection.

Extracellular enzymes, including caseinases, lipases, phospholipases, and hemolysins, play important roles in tissue degradation, membrane disruption, and nutrient acquisition during infection (Bunpa et al. 2016). In this study, isolates VA15 and VA17 exhibited the highest overall enzyme activities, consistent with their strong motility phenotypes and supporting previous observations that exoenzyme secretion may be co-regulated with flagellar gene expression and global regulatory networks (Salamone et al. 2019). Although all isolates produced detectable levels of extracellular enzymes, the magnitude of activity varied substantially among strains, suggesting isolate-specific contributions to lesion development and disease severity. Similar variability has been reported for *Vibrio* isolates from shrimp pond environments (Ayuningrum et al. 2023), and environmental factors such as nutrient availability and salinity have been shown to modulate proteolytic activity in *Vibrio* spp. (Salamone et al. 2019). The phenotypic heterogeneity observed here, therefore, likely reflects an interaction between intrinsic strain properties and environmental conditioning.

Biofilm formation among the isolates ranged from weak to moderate, consistent with previous studies reporting relatively low biofilm biomass in marine *Vibrio* species under high-salinity conditions (Mitsuwan et al. 2025). Although the absolute optical density values were lower than those typically observed in strong biofilm-forming bacteria such as *Pseudomonas* spp., biofilm production was reproducible across replicates and allowed reliable relative comparison among isolates. Even weak biofilm formation may be ecologically relevant in marine cage-culture systems by promoting environmental persistence, enhancing tolerance to antimicrobial stress, and facilitating attachment to fish mucosal surfaces. Accordingly, the observed inter-isolate variability suggests that biofilm formation, while not a dominant virulence mechanism, may contribute to persistence and transmission of *V. alginolyticus* within aquaculture environments.

β-hemolytic activity was detected in all isolates, indicating a conserved hemolytic capability among fish-pathogenic *V. alginolyticus* strains (Hernández-Robles et al. 2016). Isolates VA15 and VA17 consistently exhibited the highest hemolytic activity, in agreement with their overall high virulence phenotypic profiles. Comparable hemolytic patterns have been reported in *V. alginolyticus* isolated from marine fish and shellfish (Wei et al. 2014; Vandeputte et al. 2024). However, hemolysin expression is known to be influenced by environmental conditions and host-derived signals, suggesting that hemolysis represents an important but context-dependent component of virulence rather than a sole predictor of pathogenicity.

To integrate multiple phenotypic traits, a composite virulence score was applied as a comparative framework for ranking isolates. High-scoring isolates (≥2.2) consistently combined strong motility with elevated extracellular enzyme activity, reflecting the co-occurrence of multiple virulence-associated features. In contrast, low-scoring isolates (<1.0) were characterized by reduced motility and enzyme activity, suggesting comparatively lower virulence potential under the conditions tested. While this composite scoring approach does not provide an absolute measure of pathogenicity, it offers a practical phenotypic screening tool to prioritize isolates for subsequent molecular analyses or in vivo pathogenicity assessment.

Genetic screening revealed the universal presence of motility-associated genes (*flaA, flaC, flgE, flrA, flrB, flrC,* and *flaK*) among the screened isolates, indicating that flagellar biosynthesis represents a conserved functional pathway among the *V. alginolyticus* isolates examined in this study. These genes encode key structural and regulatory components of the flagellar apparatus (Luo et al. 2016; Echazarreta and Klose 2019), with *flaA* functioning as a central flagellin gene essential for filament assembly and swimming motility (Homma et al. 2022). The uniform detection of these genes is consistent with the strong motility phenotypes observed among the high-ranking isolates in the phenotypic assays.

The hemolysin gene profile detected (trh^+, tlh^+, tdh^-) is also consistent with patterns reported for fish-associated *V. alginolyticus* isolates in other regions, including China (Wei et al. 2014; Vandeputte et al. 2024). In contrast, *tdh*-positive strains have been reported primarily in shellfish-associated isolates from distinct geographic settings, such as Mexico (Hernández-Robles et al. 2016), highlighting host- and region-associated variation in hemolysin gene distribution. Functional studies have demonstrated that *trh* and *tlh* contribute substantially to hemolytic activity and host cell damage (González-Escalona et al. 2006; Wong et al. 2012), which is in agreement with the β-hemolytic phenotypes observed among the screened isolates in the present study.

All screened isolates also carried genes encoding components of the type III secretion system (*vopB* and *vopD*) and the type VI secretion system (*vgrG*), both of which have been implicated in host cell interactions, cytotoxicity, and interbacterial competition in *Vibrio* species (Hernández-Robles et al. 2016; Huang et al. 2024; Sun et al. 2024). In addition, the consistent detection of the siderophore-associated genes *pvsA* and *pvuA* indicates the presence of an intact vibrioferrin-mediated iron acquisition system, which is critical for bacterial survival under iron-limited conditions within the host environment (Tanabe et al. 2025).

Collectively, the uniform presence of secretion system- and iron acquisition-related genes among the screened isolates suggests that gene presence alone is insufficient to account for the observed phenotypic variability in motility, enzyme activity, and hemolysis. Instead, differences in gene regulation, expression levels, or post-transcriptional control are likely to contribute to variation in virulence-related traits among isolates. These findings underscore the importance of integrating phenotypic assays with molecular analyses and indicate that future studies incorporating gene expression profiling under host-relevant conditions would be valuable for elucidating regulatory mechanisms underlying virulence heterogeneity among *V. alginolyticus* isolates infecting farmed red drum in central Vietnam.

The pathogenicity assay demonstrated that isolate VA15 exhibits high virulence in red drum under the experimental conditions used, with an estimated LD_{50} of 4.0×10^4 CFU $fish^{-1}$. This finding is consistent with the strong in vitro virulence phenotypes and the broad repertoire of virulence-associated genes identified for this isolate. Reported LD_{50} values for *V. alginolyticus* vary widely among host species and experimental infection models, reflecting differences in host susceptibility, infection routes, and study design. For example, Mahmoud et al. (2018) reported an LD_{50} of 1.5×10^8 CFU g^{-1} body weight in sea bass (*Dicentrarchus labrax*), which is substantially higher than the value observed in red drum in the present study. In contrast, severe mortality has been reported in cobia challenged with 10^6-10^7 CFU mL^{-1} (Rameshkumar et al. 2017), while zebrafish exhibited an LD_{50} of approximately 1×10^5 CFU mL^{-1} (Muhamad-Sofie et al. 2024), only one order of magnitude higher than the estimate obtained for VA15. In combination, these comparisons indicate that the virulence expressed by *V. alginolyticus* isolates is strongly influenced by host species and experimental context, rather than reflecting a uniform pathogenic potential across hosts.

Nevertheless, the present study has certain limitations that should be considered when interpreting the results. The *in vivo* pathogenicity assessment was conducted using a single *V. alginolyticus* isolate (VA15) selected on the basis of its high in vitro virulence score, which may not fully represent the range of pathogenic potential among circulating strains in red drum farming systems. In addition, PCR-based detection of virulence-associated genes reflects gene presence but does not account for differences in gene regulation or expression during infection. Future studies incorporating multiple isolates spanning a broader range of phenotypic virulence, together with in vivo or host-relevant gene expression analyses, would help to more comprehensively elucidate the relationships between phenotype, genotype, and pathogenic outcome in *V. alginolyticus* infecting farmed red drum.

In conclusion, this study provides an integrated phenotypic and molecular characterization of *V. alginolyticus* isolates associated with hemorrhagic disease in farmed red drum in central Vietnam. Among 20 isolates examined, substantial variability was observed in swimming motility (17.33-24.33 mm), extracellular enzyme activity indices (mean 1.67-1.91), and biofilm formation (OD_{570} = 0.20-0.23). Integration of these traits into a composite virulence score revealed pronounced heterogeneity, ranging from 0.15 to 3.00, with isolate VA15 ranking highest. Although virulence-associated genes were largely conserved among high-ranking isolates—15 of 16 genes detected, with *tdh* consistently absent—gene presence alone did not explain phenotypic differences. In vivo challenge confirmed the predictive value of phenotypic profiling, as isolate VA15 caused dose-dependent mortality in red drum with an LD_{50} of 4.0×10^4 CFU $fish^{-1}$ (95% CI: 3.2×10^4-5.1×10^4 CFU $fish^{-1}$). Marked variability in motility, extracellular enzyme activity, and biofilm formation was observed among isolates, while a broad set of virulence-associated genes was consistently detected, supporting the multifactorial nature of virulence in fish-associated *V. alginolyticus*. These region-specific baseline data contribute to improved understanding of *V. alginolyticus* virulence in farmed red drum in central Vietnam and underscore the need for further studies incorporating broader sampling, multiple isolates, and in vivo gene expression analyses to elucidate better host-pathogen interactions in marine fish farming systems.

ACKNOWLEDGEMENTS

This study was funded by the Vietnamese Ministry of Education and Training under Project No. B2024-DHH-07. The authors acknowledge Hue University, Vietnam, for support through the Core Research Program (Grant No. NCTB.DHH.2025.08) and the Seed Research Grant provided by the Sydney Southeast Asia Center (SSEAC) and the Sydney Vietnam Institute (SVI).

REFERENCES

Ackerly KL, Roark KJ, Nielsen KM. 2023. Short-term salinity stress during early development impacts the growth and survival of red drum (*Sciaenops ocellatus*). Estuar Coasts 46: 541-550. https://doi.org/10.1007/s12237-022-01124-3.

Ayuningrum D, Novitasari DT, Sabdaningsih A, Jati OE. 2023. Preliminary molecular identification of proteolytic and lipolytic-enzyme producing bacteria isolated from the sediment of *Litopenaeus vannamei* pond. Asia-Pac J Mol Biol Biotechnol 31 (3): 39-49. https://doi.org/10.35118/apjmbb.2023.031.3.05.

Baker-Austin C, Oliver JD, Alam M, Ali A, Waldor MK, Qadri F, Martinez-Urtaza J. 2018. *Vibrio* spp. infections. Nat Rev Dis Primers 4: 1-19. https://doi.org/10.1038/s41572-018-0005-8.

Bardy SL, Jarrell KF. 2002. *FlaK* of the archaeon *Methanococcus maripaludis* possesses preflagellin peptidase activity. FEMS Microbiol Lett 208 (1): 53-59. https://doi.org/10.1111/j.1574-6968.2002.tb11060.x.

Bunpa S, Sermwittayawong N, Vuddhakul V. 2016. Extracellular enzymes produced by *Vibrio alginolyticus* isolated from environments and diseased aquatic animals. Procedia Chem 18: 12-17. https://doi.org/10.1016/j.proche.2016.01.002.

Del Río-Rodríguez RE, Ramírez-Paredes JG, Soto-Rodríguez SA, Shapira Y, del Jesus Huchin-Cortes M, Ruiz-Hernández J, Gomez-Solano MI, Haydon DJ. 2021. First evidence of fish nocardiosis in Mexico caused by *Nocardia seriolae* in farmed red drum (*Sciaenops ocellatus*, Linnaeus). J Fish Dis 44 (8): 1117-1130. https://doi.org/10.1111/jfd.13373.

Echazarreta MA, Klose KE. 2019. *Vibrio* flagellar synthesis. Front Cell Infect Microbiol 9: 131. https://doi.org/10.3389/fcimb.2019.00131.

González-Escalona N, Blackstone GM, DePaola A. 2006. Characterization of a *Vibrio alginolyticus* strain isolated from Alaskan oysters carrying a hemolysin gene similar to the thermostable direct hemolysin-related

hemolysin gene (*trh*) of *Vibrio parahemolyticus*. Appl Environ Microbiol 72: 7925-7929. https://doi.org/10.1128/aem.01548-06.

Hernández-Robles MF, Álvarez-Contreras AK, Juárez-García P, Natividad-Bonifacio I, Curiel-Quesada E, Vázquez-Salinas C, Quiñones-Ramírez EI. 2016. Virulence factors and antimicrobial resistance in environmental strains of *Vibrio alginolyticus*. Intl Microbiol 19 (4): 191-198. https://doi.org/10.2436/20.1501.01.277.

Homma M, Kobayakawa T, Hao Y, Nishikino T, Kojima S. 2022. Function and structure of *FlaK*, a master regulator of the polar flagellar genes in marine *Vibrio*. J Bacteriol 204: e00320-22. https://doi.org/10.1128/jb.00320-22.

Huang Z, Li Y, Yu K, Ma L, Pang B, Qin Q, Li J, Wang D, Gao H, Kan B. 2024. Genome-wide expanding of genetic evolution and potential pathogenicity in *Vibrio alginolyticus*. Emerg Microbes Infect 13 (1): 2350164. https://doi.org/10.1080/22221751.2024.2350164.

Islam MS, Rahman MZ, Khan SI, Mahmud ZH, Ramamurthy T, Nair GB, Sack RB, Sack DA. 2005. Organization of the CTX prophage in environmental isolates of *Vibrio mimicus*. Microbiol Immunol 49 (8): 779-784. https://doi.org/10.1111/j.1348-0421.2005.tb03668.x.

Li Y, Chen N, Wu Q, Liang X, Yuan X, Zhu Z, Zheng Y, Yu S, Chen M, Zhang J, Wang J, Ding Y. 2022. A flagella hook coding gene, *flgE*, positively affects biofilm formation and cereulide production in emetic *Bacillus cereus*. Front Microbiol 13: 897836. https://doi.org/10.3389/fmicb.2022.897836.

Liang H, Xia L, Wu Z, Jian J, Lu Y. 2010. Expression, characterization, and immunogenicity of flagellin *FlaC* from *Vibrio alginolyticus* strain HY9901. Fish Shellfish Immunol 29 (2): 343-348. https://doi.org/10.1016/j.fsi.2010.04.003.

Linh NQ, Yen PTH, Tram NDQ. 2022. Isolation and determination of *Vibrio* spp. pathogen from *Sciaenops ocellatus* suffering from hemorrhagic disease under cage culture in Vietnam. J Exp Biol Agric Sci 10: 405-415. https://doi.org/10.18006/2022.10(2).405.415.

Luo G, Huang L, Su Y, Qin Y, Xu X, Zhao L, Yan Q. 2016. *flrA*, *flrB,* and *flrC* regulate adhesion by controlling the expression of critical virulence genes in *Vibrio alginolyticus*. Emerg Microbes Infect 5 (1): 1-11. https://doi.org/10.1038/emi.2016.82.

Madhi M, Poursina F, Moghim S, Khademi F, Adibi P, Faghr J, Safaei HG. 2013. Recommendation of *flaA* and *flaB* as housekeeping genes in the detection of *Helicobacter pylori*. J Chem Biol Phys Sci 3: 2687-2696.

Mahmoud SA, El-Bouhy ZM, Hassanin ME, Fadel AH. 2018. *Vibrio alginolyticus* and *Photobacterium damselae* subsp. Damsel: Prevalence, histopathology, and treatment in sea bass *Dicentrarchus labrax*. J Pharm Chem Biol Sci 5 (4): 354-364.

Ministry of Agriculture and Rural Development (MARD). 2021. Decision No. 1644/QĐ-TTg dated October 4, 2021: Scheme on Marine Aquaculture Development to 2030, With a Vision to 2045. Ministry of Agriculture and Rural Development, Hanoi, Vietnam. Available from: https://vanban.chinhphu.vn/default.aspx?pageid=27160&docid=204234.

Mitsuwan W, Boripun R, Saengsawang P, Intongead S, Boonplu S, Chanpakdee R, Morita Y, Boonmar S, Rojanakun N, Suksriroj N, Ruekaewma C, Tenitsara T. 2025. Multidrug resistance, biofilm-forming ability, and molecular characterization of *Vibrio* species isolated from foods in Thailand. Antibiotics 14 (3): 235. https://doi.org/10.3390/antibiotics14030235.

Mmanda FP, Zhou S, Zhang J, Zheng X, An S, Wang G. 2014. Massive mortality associated with *Streptococcus iniae* infection in cage-cultured red drum (*Sciaenops ocellatus*) in eastern China. Afr J Microbiol Res 8: 1722-1729. https://doi.org/10.5897/ajmr2014.6659.

Movaghari M, Anvari S, Jamali A, Yazdani M. 2017. Detection of *tcpA* and *ctxB* virulence genes in isolates from surface waters and salt waters in Golestan, Iran. Med Lab J 11 (3): 25-29. https://doi.org/10.18869/acadpub.mlj.11.3.25.

Muhamad-Sofie MHN, Mohamad A, Azzam-Sayuti M, Amal MNA, Zamri-Saad M, Monir MS, Yasin ISM. 2024. Stability and efficacy of live-attenuated *Vibrio harveyi* vaccines under different storage conditions in Zebrafish (*Danio rerio)* models. Jurnal Ilmiah Perikanan dan Kelautan 16 (2): 322. https://doi.org/10.20473/jipk.v16i2.59794.

Park SB, Zhang Y. 2024. Innovative multiplex PCR assay for detection of *tlh*, *trh*, and *tdh* genes in *Vibrio parahemolyticus* with reference to the U.S. FDA's Bacteriological Analytical Manual (BAM). Pathogens 13 (9): 774. https://doi.org/10.3390/pathogens13090774.

Partridge JD. 2022. Surveying a swarm: Experimental techniques to establish and examine bacterial collective motion. Appl Environ Microbiol 88: e01853-21. https://doi.org/10.1128/aem.01853-21.

Phuoc NN, Hong NTX, Chung NC. 2020. Study on the virulence of some *Vibrio parahemolyticus* strains causing Acute Hepato-Pancreatic Necrosis Disease (AHPND) in whiteleg shrimp (*Litopenaeus vannamei*) cultured in Thua Thien Hue. Vietnam J Agric Sci 18 (3): 202-211. [Vietnamese]

Rameshkumar P, Nazar AKA, Pradeep MA, Kalidas C, Jayakumar R, Tamilmani G, Sakthivel M, Samal AK, Sirajudeen S, Venkatesan V, Nazeera BM. 2017. Isolation and characterization of pathogenic *Vibrio alginolyticus* from sea cage cultured cobia (*Rachycentron canadum* (Linnaeus 1766)) in India. Lett Appl Microbiol 65 (5): 423-30. https://doi.org/10.1111/lam.12800.

Reed LJ, Muench H. 1938. A simple method of estimating fifty percent endpoints. Am J Hyg 27: 493-497.

Salamone M, Nicosia A, Ghersi G, Tagliavia M. 2019. *Vibrio* proteases for biomedical applications: Modulating the proteolytic secretome of *Vibrio alginolyticus* and *Vibrio parahemolyticus* for improved enzyme production. Microorganisms 7 (10): 387. https://doi.org/10.3390/microorganisms7100387.

Sheikh HI, Alhamadin NII, Liew HJ, Fadhlina A, Wahid MEA, Musa N, Jalal KCA. 2024. Virulence factors of the zoonotic pathogen *Vibrio alginolyticus*: A review and bibliometric analysis. Appl Biochem Microbiol 60: 514-531. https://doi.org/10.1134/s0003683823602822.

Stepanović S, Vuković D, Dakić I, Savić B, Švabić-Vlahović M. 2000. A modified microtiter-plate test for quantification of staphylococcal biofilm formation. J Microbiol Methods 40 (2): 175-179. https://doi.org/10.1016/S0167-7012(00)00122-6.

Sun Y, Yan Y, Yan S, Li F, Li Y, Yan L, Yang D, Peng Z, Yang B, Sun J, Xu J, Dong Y, Bai Y. 2024. Prevalence, antibiotic susceptibility, and genomic analysis of *Vibrio alginolyticus* isolated from seafood and freshwater products in China. Front Microbiol 15: 1381457. https://doi.org/10.3389/fmicb.2024.1381457.

Tanabe T, Hori M, Kimura N, Tadokoro R, Nagaoka K, Funahashi T. 2025. Identification of genes involved in the utilization of hydroxamate xenosiderophores in *Vibrio alginolyticus*. BPB Rep 8 (1): 9-17. https://doi.org/10.1248/bpbreports.8.1_9.

Vandeputte M, Coppens S, Bossier P, Vereecke N, Vanrompay D. 2024. Genomic mining of *Vibrio parahemolyticus* highlights the prevalence of antimicrobial resistance genes and new genetic markers associated with AHPND and tdh^+/trh^+ genotypes. BMC Genomics 25: 178. https://doi.org/10.1186/s12864-024-10093-9.

Wei S, Zhao H, Xian Y, Hussain MA, Wu X. 2014. Multiplex PCR assays for the detection of *Vibrio alginolyticus*, *Vibrio parahemolyticus*, *Vibrio vulnificus*, and *Vibrio cholerae* with an internal amplification control. Diagn Microbiol Infect Dis 79 (2): 115-118. https://doi.org/10.1016/j.diagmicrobio.2014.03.012.

Wong SK, Zhang X-H, Woo NYS. 2012. *Vibrio alginolyticus* Thermo-Labile Hemolysin (TLH) induces apoptosis, membrane vesiculation, and necrosis in sea bream erythrocytes. Aquaculture 330-333: 29-36. https://doi.org/10.1016/j.aquaculture.2011.12.012.

Xiao Y, Liu J, Wei J, Xiao Z, Li J, Aguilar-Perera A, Herrera-Ulloa A. 2023. Future climate change accelerates the invasive rhythm of alien marine species: New insights into the invasive potential of the world's aquaculture species, red drum (*Sciaenops ocellatus*). Ecol Indic 155: 111069. https://doi.org/10.1016/j.ecolind.2023.111069.

Yen PTH, Linh NQ, Tram NDQ. 2021. Identification and determination of toxin genes of *Vibrio* strains causing hemorrhagic disease in red drum (*Sciaenops ocellatus*) using PCR. AMB Express 11: 4. https://doi.org/10.1186/s13568-020-01161-w.